A New Tensegrity Module – "Torus"

Xingfei Yuan*, Zhangli Peng, Shilin Dong and Baojun Zhao

Space Structures Research Center, Zhejiang University, Hangzhou 310027, China

(Received: 6 August 2007; Received revised form: 19 November 2007; Accepted: 28 February 2008)

Abstract: Research on cylindrical and spherical tensegrity modules are extensively carried out. However research on other tensegrity modules is little reported. This paper presents an exploratory study on a new kind of tensegrity module – "torus". The topology of the torus tensegrity is firstly introduced. Then the initial form-finding of the torus tensegrity is discussed. The static and dynamic analysis of the torus tensegrity shows that prestressing has a stiffening effect on infinitesimal mechanism modes if the geometry is properly arranged. A new cable dome with a torus tensegrity employed as its ring beam is finally proposed. The behavior of the new dome is also examined. The work here will provide a reference for further research and application of the torus tensegrity.

Key words: tensegrity, torus, form-finding, cable dome, ring beam.

1. INTRODUCTION

Tensegrity structures are a class of truss structures consisting of a continuous set of cables (tension members) and a discrete set of struts (compression members). The word *tensegrity* was a contraction of *tensile* and *integrity*, first conceived by Fuller (1962). With artists' work as the starting point, much research work on different types of tensegrity modules and systems has been carried out during the past 70 years.

Cylindrical and spherical tensegrity modules are two basic modules extensively studied. The cylindrical tensegrity as shown in Figure 1(a) was created by Snelson and applied in the "Needle Tower" as an artwork displayed at the Hirshhorn Museum of Modern Art, Washington, DC. By incorporating Snelson's work into geodesics, Fuller developed a regular spherical tensegrity module as shown in Figure 1(b) and then proposed a geodesics dome. A construction method of truncated spherical tensegrity modules was first introduced by Pugh (1976). By using a symbolic manipulator, Sultan (1999) performed static and dynamic analyses of cylindrical tensegrity modules. The initial shape-finding and modal analysis of cyclic frustum tensegrity modules was also presented by Nishimura and Murakami (2001). However, no other tensegrity module has been reported. Are there other basic tensegrity modules? Since cylindrical and spherical tensegrity modules are modules corresponding to basic geometry - cylinder and sphere respectively, modules corresponding to other geometry might exist. The torus tensegrity proposed herein is such a new kind of basic module which has its inspiration in the basic ring geometry.

This paper presents a primary study of the torus tensegrity as shown in Figure 1(c). The layout of the paper is as follows. The topology of the torus tensegrity is firstly introduced in Section 2. By taking a simple four-segment torus tensegrity with three struts per segment as an example, the construction procedure is illustrated. Following that, the form-finding analysis of the torus tensegrity including the determination of prestressing and infinitesimal mechanism modes and the validation of geometric stability is carried out in Section 3. The static and dynamic analysis is then conducted in Section 4. By employing a torus tensegrity as the ring beam, a new tensegrity cable dome is proposed and the preliminary behavior of the new dome is examined in Section 5. Some conclusions are finally obtained in Section 6.

*Corresponding author. Email address: yuanxf@zju.edu.cn; Fax and Tel: +86-571-8795-2414.

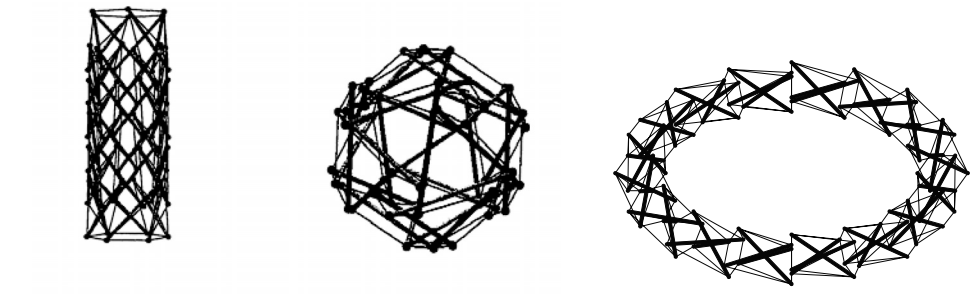

(a) Cylindrical Tensegrity (b) Spherical Tensegrity (c) Torus Tensegrity

Figure 1. Tensegrity modules

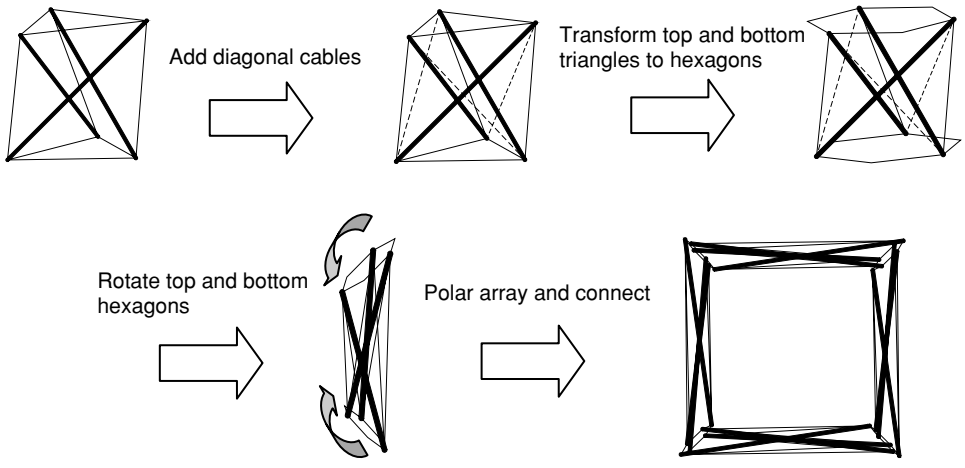

Figure 2. Construction of a four-segment torus tensegrity with three struts per segment

2. TOPOLOGY

Snelson's tensegrity module is created by assembling tensegrity prisms on top of each other. Similarly the torus tensegrity can be constructed by placing modified tensegrity prisms on top of each other along a circle. To illustrate the construction procedure, a four-segment tensegrity torus with three struts per segment as shown in Figure 2 is taken as an example. The first step is to add diagonal cables to each face of the prism. In order to avoid the touching of struts when two prisms are connected, the top and bottom m sides polygons are then transformed to $2m$ sides polygons. To be connected as a torus, the top and bottom polygons should be inversely rotated with respect to the longitudinal axis though the center of the torus in a certain angle. Connecting these modified prisms in polar array can then produce a torus tensegrity. In the figures, bold lines denote struts and thin and dash lines denote cables.

The topology of the torus tensegrity can be described in a connectivity diagram where number of nodes and elements are labeled clearly (Figure 3). Similar diagram was first proposed by Pugh (1976) to illustrate a building method for tensegrity modules. Cables can be divided according to their different positions into base cables, straight cables and diagonal cables. If the number of the segments is n and the number of the struts per segment is m, then that torus tensegrity can be denoted as T(n-m). The torus tensegrity with different number of segments and struts per segment are shown in Figure 4. Construction procedure of torus tensegrity T (16-3) is shown in Figure 5.

It can be seen that a torus tensegrity possesses cyclic symmetry. Every two segments in a torus tensegrity are congruent. Therefore, if one rotates the module with respect to the longitudinal axis though the center of the torus by $4\pi/n$, the resulting configuration is exactly the same as before. Twist angle θ between top and bottom polygons in each tensegrity prism is a very important parameter in a torus tensegrity. Based on numerical analyses, it is found that only when the value of θ is within a certain range can the torus tensegrity be built successfully or becomes prestressable, that is, the shape of the torus tensegrity can be maintained with force interactions only between cables and struts and no

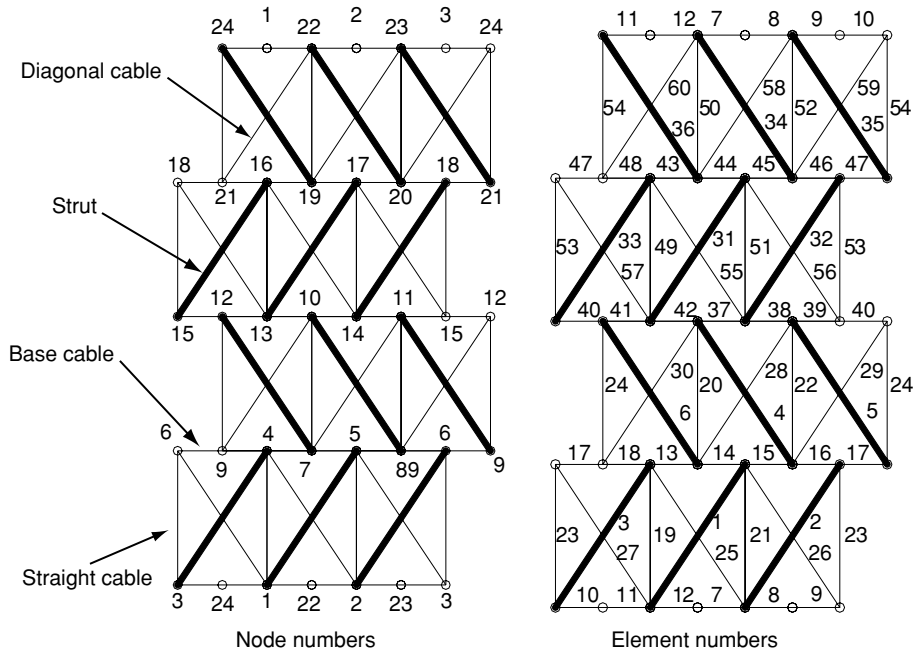

Figure 3. Connectivity diagram of the torus tensegrity *T*(4-3)

Figure 4. The torus tensegrity with an arbitrary number of stages

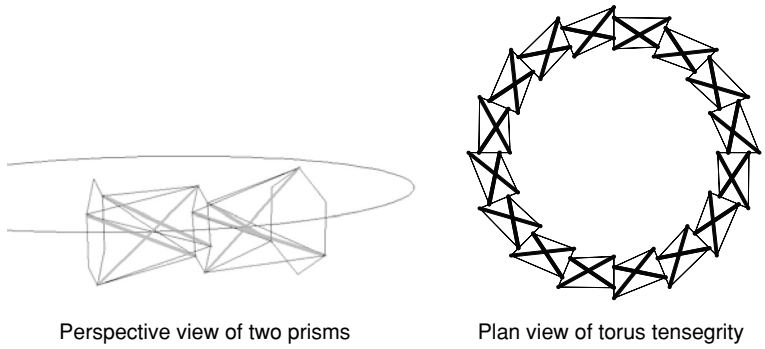

Figure 5. Composition diagram of the torus tensegrity *T*(16-3)

externally applied loads. This fundamental property of tensegrity structures is called prestressability. With other twist angles, prestressability conditions cannot be satisfied and the shape of the torus tensegrity cannot be maintained.

3. FORM-FINDING

3.1. General Form-Finding Analysis

Form-finding is a preliminary process to study tensegrity systems, during which the prestressing is determined and the self-equilibrating configuration is fulfilled. To obtain

the initial configuration that satisfies a prestressability condition, the static and kinematic property should be discussed.

The Maxwell number M_x defined in terms of both the number of nodes and elements is often used to predict the response of trusses as stiff structures or as unstable mechanisms (Maxwell 1864). When $M_x > 0$, the truss is redundant and statically indeterminate. When $M_x = 0$, the truss is statically determinate. When $M_x < 0$, the truss is a kinematically indeterminate mechanism. As exceptions to $M_x < 0$, Maxwell predicted the existence of tensegrity-type structures that exhibit stiffness on the order of prestressing, instead of element stiffness due to Young's modulus. Calladine (1978) also observed that most tensegrity structures possess infinitesimal mechanisms that could be stiffened by prestressing to exhibit Maxwell's "inferior-order stiffness". He then obtained the relationship between the number of prestressing modes s and the number of mechanism k as $s\text{-}k = M_x$, which is also referred to as the extended Maxwell's rule.

In order to compute the Maxwell number of the torus tensegrity, it is necessary to count the number of nodes and elements. To this end, the connectivity diagrams prove to be useful. Consider an n-segment torus tensegrity with m struts per segment, each segment has m bars, $2m$ base cables to form the regular m-sided polygons at the two ends, $2m$ straight and diagonal cables connected between the two polygons and $2m$ joints. Therefore, the number of total elements and total joints in a torus tensegrity are $5mn$ and $2mn$ respectively. With 6 constraints to remove the rigid motions, the Maxwell's rule yields $M_x = 6\text{-}3(2mn) + 5mn = 6\text{-}mn < 0$ ($m \geq 3$, $n \geq 4$). According to the extended Maxwell rule, the relationship between the number of prestressing modes and the number of mechanism is obtained as $s\text{-}k = 6\text{-}mn$. This shows that the torus tensegrity is kinematically indeterminate.

To obtain the prestressing and mechanism modes, the Singular Value Decomposition (SVD) of the initial equilibrium matrix should be carried out. It involves equilibrium matrix theory developed by Pellegrino and Calladine (1986, 1991, 1993). The equilibrium equation of the torus tensegrity when the external loads are zero can be expressed as follows.

$$\mathbf{At} = 0 \tag{1}$$

where $\mathbf{A}$ is the initial equilibrium matrix and $\mathbf{t}$ is the stress vector of elements. Once the initial configuration is determined, infinitesimal mechanism and prestressing modes can be numerically obtained from the subspaces of the known equilibrium matrix $\mathbf{A}$ which are obtainable with SVD.

The next work is to judge if feasible prestressing modes exist, which satisfy the condition that cables are subject to tension and struts subject to compression. If there exists no feasible self-stress mode, it indicates the geometric is unreasonable and the topology or geometry should be rearranged. If there exists feasible self-stress modes and infinitesimal mechanism modes, the geometrical stability of the torus tensegrity should be further examined by using a method based on product-force vectors developed by Pellegrino (1993) or the modal analysis described in Section 4 to see if the prestressing has a stiffening effect on infinitesimal mechanism modes. A set of the above general procedures for form-finding of the torus tensegrity is shown in Figure 6.

3.2. Form-Finding of Torus Tensegrity T(4-3)

The torus tensegrity *T(4-3)* as shown in Figure 2 is taken as an example. In order to compute the Maxwell number, it is necessary to count the number of nodes and elements according to the connectivity diagram as shown in Figure 3. It is easy to see the Maxwell number $M_x = 6\text{-}mn = -6$, and thus $s\text{-}k = -6$.

As shown in Figure 3, there are 24 nodes and 60 elements in the torus tensegrity. In order to define nodal coordinates of the the torus tensegrity, a Cartesian coordinate system {x, y, z} is employed with the origin at the center of the torus. Let the average value of outer and inner radii of the torus, the radii of inscribing circles of regular polygons, the twist angle and the central angle of each segment be denoted by R_t, r, θ and α respectively, and coordinates of nodes 1-6 can be expressed as follows.

$$x_1 = (R_t + r\cos 0)\cos 0 = R_t + r$$

$$x_2 = \left(R_t + r\cos\frac{2\pi}{3}\right)\cos 0 = R_t - 0.5r$$

$$x_3 = \left(R_t + r\cos\frac{4\pi}{3}\right)\cos 0 = R_t - 0.5r$$

$$x_4 = (R_t + r\cos\theta)\cos\alpha$$

$$x_5 = \left[R_t + r\cos\left(\frac{2\pi}{3} + \theta\right)\right]\cos\alpha$$

$$x_6 = \left[R_t + r\cos\left(\frac{4\pi}{3} + \theta\right)\right]\cos\alpha$$

$$y_1 = (R_t + r\cos 0)\sin 0 = 0$$

$$y_2 = \left(R_t + r\cos\frac{2\pi}{3}\right)\sin 0 = 0$$

$$y_3 = \left(R_t + r\cos\frac{4\pi}{3}\right)\sin 0 = 0$$

$$y_4 = (R_t + r\cos\theta)\sin\alpha$$

$$y_5 = \left[R_t + r\cos\left(\frac{2\pi}{3} + \theta\right)\right]\sin\alpha$$

$$y_6 = \left[R_t + r\cos\left(\frac{4\pi}{3} + \theta\right)\right]\sin\alpha$$

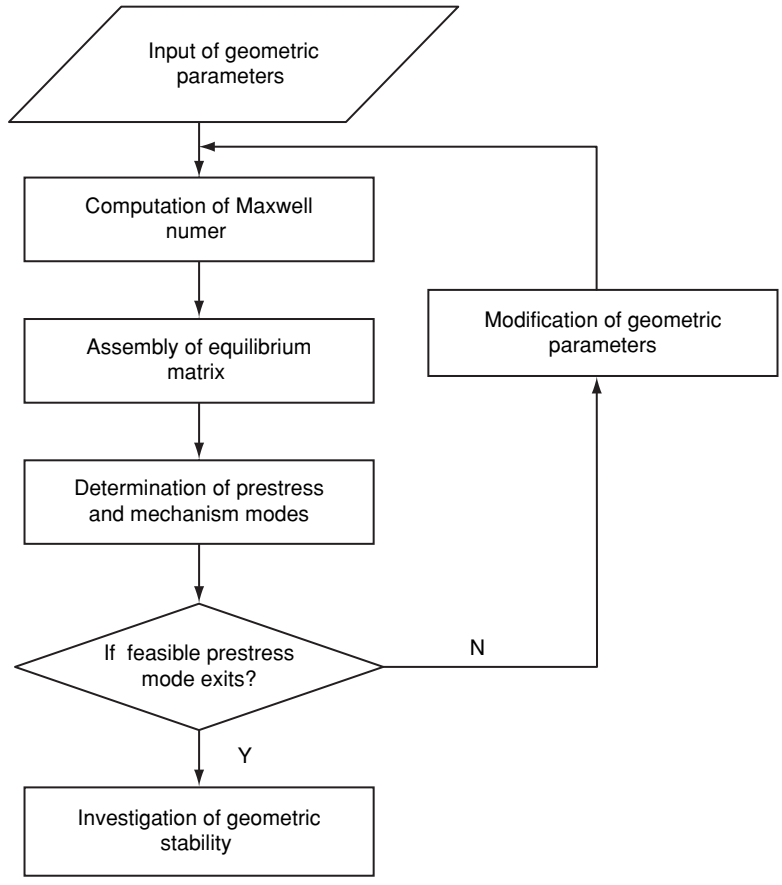

Figure 6. General procedure for form-finding analysis of the torus tensegrity

$$z_1 = r\sin 0 = 0$$
$$z_2 = r\sin\frac{2\pi}{3} = \sqrt{3}r/2$$
$$z_3 = r\sin\frac{4\pi}{3} = -\sqrt{3}r/2$$
$$z_4 = r\sin\theta$$
$$z_5 = r\sin(\frac{2\pi}{3}+\theta)$$
$$z_6 = r\sin(\frac{4\pi}{3}+\theta)$$

Let $R_t = 3m$, $r = 0.5m$, $\theta = \frac{\pi}{3}$ and $\alpha = \frac{2\pi}{n} = \frac{\pi}{2}$, coordinates of node 1-6 have the following values.

$x_1 = 3.5$	$y_1 = 0$	$z_1 = 0$
$x_2 = 2.75$	$y_2 = 0$	$z_2 = 0.433$
$x_3 = 2.75$	$y_3 = 0$	$z_3 = -0.433$
$x_4 = 0$	$y_4 = 3.25$	$z_4 = 0.433$
$x_5 = 0$	$y_5 = 2.5$	$z_5 = 0$
$x_6 = 0$	$y_6 = 3.25$	$z_6 = -0.433$

Coordinates of other nodes can be obtained by coordinate transformation.

The equilibrium matrix **A** of the *T(4-3)* torus tensegrity has dimension 72 × 60. By SVD of **A**, it can be obtained that the rank of **A** is 58 and the number of the independent self-stress mode s is 2. The detail independent self-stress modes can be denoted as t_1 and t_2. By combining the two independent self-stress modes, the general self-stress mode $\boldsymbol{t}_0$ can be obtained as follows

$$\boldsymbol{t}_0 = \boldsymbol{c}_1\boldsymbol{t}_1 + \boldsymbol{c}_2\boldsymbol{t}_2$$

where $\boldsymbol{c}_1$ and $\boldsymbol{c}_2$ are the participation coefficients of the independent self-stress mode. With $c_1 = 1$ and $c_2 = 0$, a feasible self-stress mode can be obtained, which satisfies the condition that cables are in tension and struts in compression.

Since the rank of **A** is 58, the number of internal mechanism inextensional modes $k = 72 - 58 - 6 = 8$. This also agrees with Calladine's rule, that is, $s - k = 2 - 8 = -6 = M_x$. The first two internal infinitesimal mechanism modes are illustrated in Figure 7. The first mode exhibits the horizontal movement like a planar four-bar mechanism. The second mode shows the vertical movement. In the figures, dashed lines show the undeformed configurations.

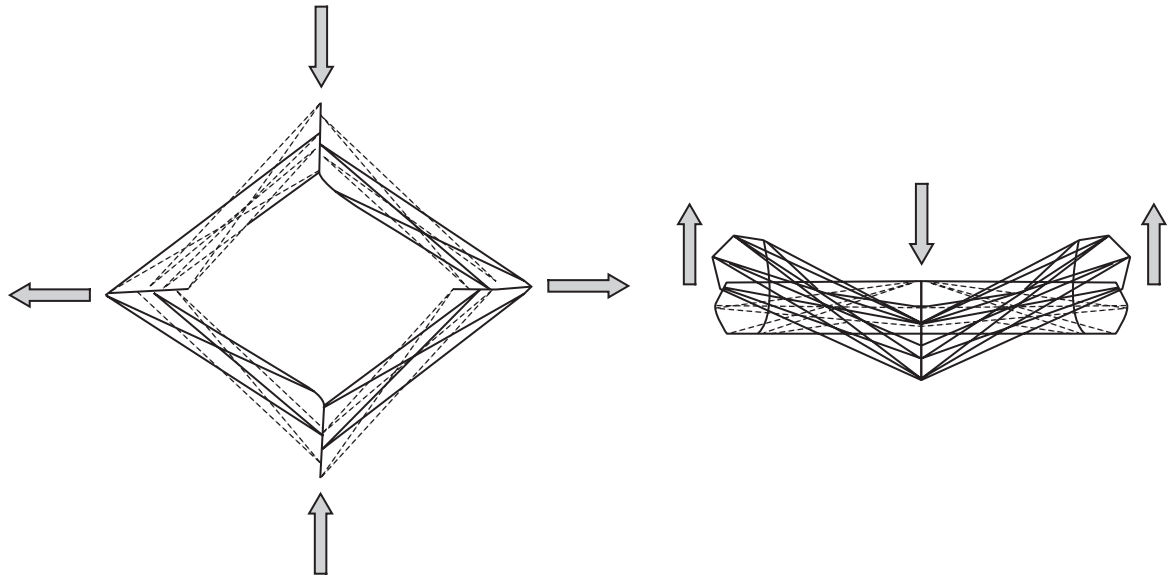

Figure 7. First two internal mechanism modes of T(4-3)

Further geometrical stability analysis of the torus tensegrity shows that prestressing stabilizes the infinitesimal mechanisms, and hence, the structure by providing stiffness.

4. STATIC AND DYNAMIC CHARACTERISTIC OF TORUS TENSEGRITY

For a complete analysis of the torus tensegrity, its static and dynamic properties must be investigated. The load deflection characteristic of the torus tensegrity described in Section 3 is first examined. The geometric parameters are assumed as $R_t = 3m$, $r = 0.5m$, and $\theta = \pi/3$. The cross sectional areas of cables and struts are 1 cm^2 and 10.21cm^2 respectively. The Young's modulus of struts and cables are 2e11N/m^2 and 1.85e11N/m^2 respectively. Six constraints including three in z-direction, two in x-direction and one in y-direction are introduced into the torus tensegrity to prevent the rigid-body displacements of the structure.

A general prestressing mode can be expressed as follows.

$$
\begin{aligned}
t^{\mathrm{T}} = p[&-0.2303\ -0.2326\ -0.2326\ -0.2326\ -0.2303\ -0.2326\\
&0.0399\ 0.0365\ 0.0365\ 0.0399\ 0.0432\ 0.0432\\
&0.0399\ 0.0365\ 0.0365\ 0.0399\ 0.0432\ 0.0432\\
&0.0988\ 0.1164\ 0.1275\ 0.1275\ 0.1164\ 0.0988\\
&0.1164\ 0.1275\ 0.0988\ 0.1275\ 0.1164\ 0.0988\\
&0.0399\ 0.0365\ 0.0365\ 0.0399\ 0.0433\ 0.0433]
\end{aligned}
$$

where p is the prestressing level and here taken as 400kN. Two load cases are considered. In the first case, each node on the middle polygon of the torus is subjected to a vertical load of 100N as shown in Figure 8. In the second load case, each node on the middle polygon is subjected to a horizontal load of 100N as shown in Figure 9. The load-displacement relationship is investigated by using the updated Lagrangian method. The maximum displacement of the structure under vertical and horizontal load is 0.71m and 0.21m respectively. From the corresponding load - displacement curves illustrated in Figure 10, it can be seen that the relationship between load and displacement is nearly linear, which shows the illustrative torus tensegrity has good global stiffness with the initial prestressing. In fact, the stiffness of the torus tensgrity is not only related to the level of prestressing force, but also related to topology and geometry.

The natural frequencies of a structure are perhaps the most essential characteristics in determining the dynamic behavior of the structure. The equilibrium equations for the free vibration of an undamped multiple degree of freedom system can be defined as a set of linear homogeneous second-order ordinary differential equations as (Clough 1993)

$$M\ddot{U} + KU = 0 \tag{2}$$

where U is the nodal displacement vector; $\ddot{U}$ is the nodal acceleration vector; K is the tangent stiffness matrix and M is the mass matrix. To a prestressed structure, the stiffness K is decomposed into the initial stiffness K_0 employed for small-deformation truss analyses and the stiffness K_g induced by prestressing.

Assuming a harmonic motion for the temporal displacement, the solution of Eqn 2 is obtained as a set of linear homogeneous algebraic equations shown as

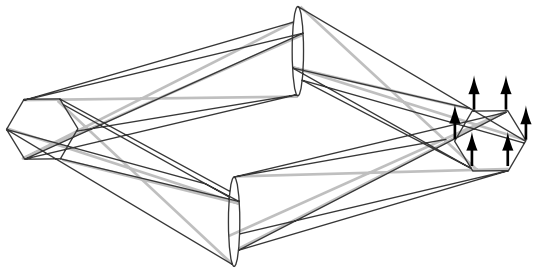

Figure 8. *T*(4-3) under vertical loads

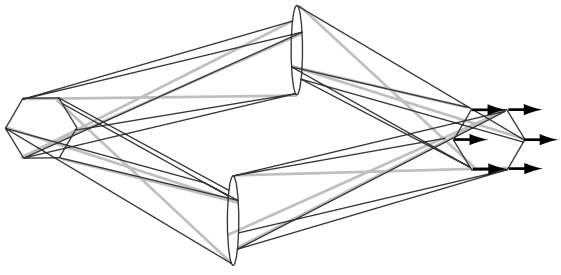

Figure 9. *T*(4-3) under horizontal loads

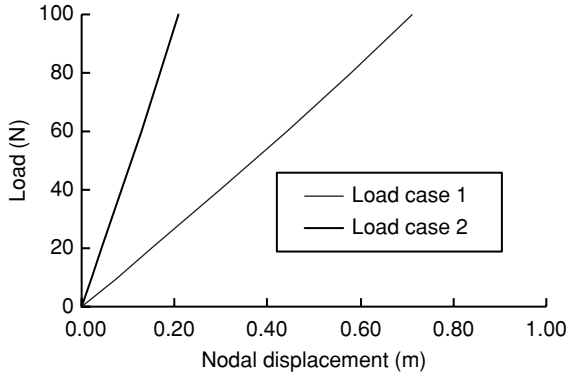

Figure 10. Load-displacement curves of *T*(4-3)

$$K\Phi = \omega^2 M\Phi \tag{3}$$

The above equation is mathematically known as a generalized eigen value problem between the stiffness and mass matrices of the system. The values of ω are the circular frequencies and the vectors of Φ are the corresponding mode shapes.

In order to clarify the effect of prestressing, natural frequencies are computed for three prestressing levels of $p = 4$kN, $p = 40$kN and $p = 400$kN. The eigen problem is solved numerically by using the Jacobi method. Table 1 gives out the natural frequencies with increasing prestressing amplitude. The first ten natural frequencies of infinitesimal mechanism modes increase approximately in proportion to the square root of the amplitude of prestressing. The natural frequencies higher than the tenth do not change significantly with increasing prestressing levels. It shows the stiffness of the first ten modes are largely dependent on the order of prestressing, while that of the higher order modes are dependent on the order of Young's modulus and prestressing together.

Table 1. Natural frequencies of the torus tensegrity with increasing prestressing amplitude

Mode	$p = 4$kN	$p = 40$kN	$p = 400$kN
First	0.109	0.328	1.072
Second	0.150	0.449	1.437
Third	0.724	2.285	7.367
Fourth	0.816	2.581	8.534
Fifth	1.108	3.197	9.991
Sixth	1.257	3.401	10.640
Seventh	1.257	3.503	11.572
Eighth	1.436	3.974	13.001
Ninth	1.508	3.974	13.001
Tenth	1.634	5.135	14.049
Eleventh	9.264	9.763	14.049
Twelfth	9.264	9.763	15.137

5. A NEW CABLE DOME SYSTEM

The most successful application of tensegrity system in building structures is the cable dome, first proposed by Geiger and first employed in the roofs for the Olympic Gymnastics Hall and the Fencing Hall in Seoul (Geiger 1986). Due to their innovative forms and lightweight, cable domes have become popular as roofs for structures including arenas, stadiums and sport centers over the past two decades. The largest existing dome - Georgia Dome (Levy 1994), with an elliptical plan, was designed for Atlanta Olympic Games in 1996.

There is no consensus on the definition of cable domes. The main divergence lies in the boundary compression ring of the cable dome, which is something inconsistent with the self-support definition of tensegrity system. Studies on tensegrity structures as ring beams have been carried out by Wang Bin-bing (1996) where tensegrity prismatic or pyramidal simplices were radially linked to form a tensegrity ring beam.

Employing a torus tensegrity as the ring beam of a traditional cable dome will generate a new cable dome system as shown in Figure 11. In this system, the cable dome and the torus tensegrity interact as a whole structure, forming an exactly "free standing, self stressed and self equilibrium" tensegrity system.

A new Levy dome with a torus tensegrity employed as its ring beam is shown in Figure 12. The dome is divided into 12 sections in the latitudinal direction and has 3 cable hoops. The torus tensegrity is composed of 12 segments with geometric parameters $R_t = 50m$ and $r = 4m$. The cross sectional areas of struts and cables in the cable dome are 0.05m^2 and 0.005m^2 respectively.

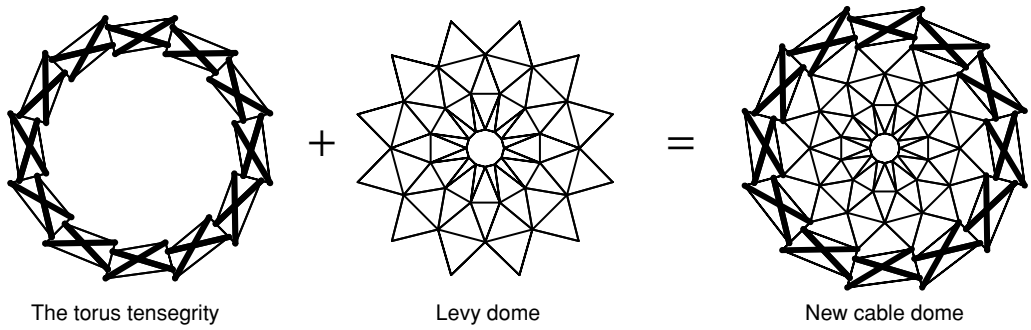

Figure 11. New cable dome system

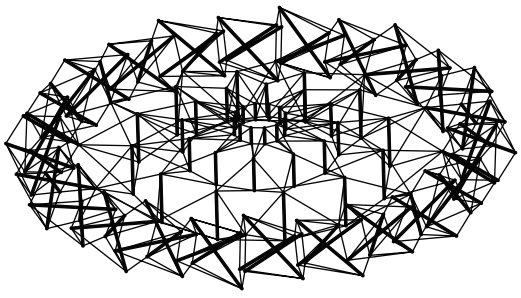

Figure 12. Three-dimensional view of the new tensegrity cable dome

The cross sectional areas of struts and cables in the torus tensegrity are $0.1m^2$ and $0.01m^2$ respectively. The Young's modulus of struts and cables are $2e11N/m^2$ and $1.85e11N/m^2$ respectively. The structure is subject to a uniformly distributed vertical load $q = 0.5kN/m^2$. Vertical constraints in the bottom nodes of the torus tensegrity and horizontal constraints in several nodes are provided to prevent rigid body motion of the whole structure. Considering the symmetry of the dome, the members in the same family possess equal prestressing (Yuan 2003). The prestressing mode of the torus tensegrity $\boldsymbol{t}_t$ and that of the cable dome $\boldsymbol{t}_c$ are obtained by using SVD method, as listed as follows.

$\boldsymbol{t}_t^T$ = [–0.1266 –0.1275 –0.1275 –0.1275 –0.1266
–0.1275 0.0501 0.0460 0.0460 0.0501
0.0541 0.0541 0.0501 0.0460 0.0460 0.0501
0.0541 0.0541 0.0491 0.0578 0.0639 0.0639
0.0578 0.0491 0.0578 0.0639 0.0491 0.0639
0.0578 0.0491]

$\boldsymbol{t}_c^T$ = [–0.0048 –0.0144 –0.0325 0.0579 0.0878
0.1340 0.0292 0.0456 0.0726 0.0558 0.0837
0.1255 0.1116]

The maximum initial prestressing of cables are taken as 640 MPa according to the material strength and the structural safety. Through nonlinear finite element analysis, the behavior of the new dome is studied. Numerical results show the stress of cables and struts are lower than the allowable stress of material and no cables are slack. The maximum vertical displacement in the mid-span can be obtained as follows.

$$U_{zmax} = 0.167m \approx 50m/300$$

Modal analysis is also conducted and it is found that the natural frequencies of the new cable dome are very closely distributed. The first thirteen modes of the structure are local vibration of cables and struts. The modes are global vibrations from the fourteenth order with a value of 3.41Hz.

Both static and modal analysis shows that the proposed new cable dome system with proper prestressing has large global stiffness and load resistance capacity.

6. CONCLUSIONS

Based on the theoretical and numerical analyses above, we may have the following conclusions. A torus tensegrity is a feasible type of tensegrity. If the geometric is properly arranged, then prestressing has a stiffening effect on infinitesimal mechanisms and makes the structure geometrically stability. Employing a torus tensegrity as the ring beam, a new cable dome is proposed and the behavior is investigated. With good static and dynamic characteristic, a tensegrity cable dome satisfying the condition of free standing, self stressed and self equilibrium is conceived. Further work includes the determination of feasible twist angle θ of the torus tensegrity and the connection between the torus tensegrity and the traditional cable dome. The optimum of prestressing level and the detail dynamic behavior are also good research topics.

ACKNOWLEDGEMENTS

The authors are grateful to the National Natural Science Foundation of China for supporting this work (Grant No. 50638050).

REFERENCES

Calladine, C.R. (1978). "Buckinster Fuller's "tensegrity" structures and Clerk Maxwell's rules for the construction of stiff frames", *International Journal of Solids and Structures,* Vol. 14, No. 2, pp. 161–172.

Clough, R.W. and Penzien, J. (1993). *Dynamics of Structures,* McGraw-Hill, New York, UK.

Fuller, RB. (1962). *Tensile-integrity Structures,* U.S, Patent 3063521.

Geiger, D.H., Stenfaniuk, A. and Chen, D. (1986). "The design and construction of two cable domes for the Korean Olympics", *Proceedings of International Association of Space Structures-American Society of Civil Engineers,* Osaka, Japan, Vol. 2, pp. 265–272.

Levy, M.P. (1994). "The Georgia dome and beyond achieving light weight-long span structures", *Proceedings of International Association of Space Structures-American Society of Civil Engineers*, Atlanta, USA, pp. 560–562.

Maxwell, J.C. (1864). "On the calculation of the equilibrium and stiffness of frames", *Philosophical Magazine*, Vol. 27, No. 7, pp. 294–299.

Nishimura, Y. and Murakami, H. (2001). "Initial shape-finding and modal analyses of cyclic frustum tensegrity modules", *Computer Methods in Applied Mechanics and Engineering*, Vol. 190, No. 43-44, pp. 5795–5818.

Pellegrino, S. and Calladine, C.R. (1986). "Matrix analysis of statically and kinematically indeterminate frameworks", *International Journal of Solids and Structures*, Vol. 22, No. 4, pp. 409–428.

Pellegrino, S. and Calladine, C.R. (1991). "First-order infinitesimal mechanisms", *International Journal of Solids and Structures*, Vol. 27, No. 4, pp. 505–515.

Pellegrino, S. (1993). "Structural computations with the singular value decomposition of the equilibrium matrix", *International Journal of Solids and Structures*, Vol. 30, No. 21, pp. 3025–3035.

Pugh, A. (1976). *An Introduction to Tensegrity*, University of California Press, Berkeley, CA.

Sultan, C. (1999). *Modeling, Design, and Control of Tensegrity Structures with Applications*, PhD Thesis, Purdue University, West Lafayette, India.

Wang, B. (1996). "Tensegrity structures as 'ring beams'", *Journal of the International Association for Shell and Spatial Structures*, Vol.37, No.120, pp. 31–38.

Yuan, X.F. and Dong, S.L. (2003). "Integral feasible prestress state of cable domes", *Computers & Structures*, Vol. 81, No. 21, pp. 2111–2119.